Comparative Kinetics of the Induced Radical Autocondensation of Polyflavonoid Tannins. II. Flavonoid Units Effects

E. MASSON,[1,2] A. PIZZI,[1] M. MERLIN[2]

[1] ENSTIB, University of Nancy 1, Epinal, France

[2] Laboratory of Applied Photochemistry, University of Nancy 1, Nancy, France

Received 13 July 1995; accepted 15 September 1996

ABSTRACT: Comparative kinetics of the radical autocondensation induced by SiO_2 on a series of polyflavonoid tannins, namely, pine, pecan, mimosa, quebracho, gambier, sumach, and on the catechin monomer as a model compound were carried out by electron spin resonance. The induced radical autocondensation appeared to be independently catalyzed by the known base mechanism, as well as SiO_2 and Lewis acid attack directly at the heterocycle oxygen. The reaction occurs in two definite steps: the first, the radical-anion formation, the second, the condensation proper with other flavonoid units of the reactive sites formed. The rate determining step depends on both the main flavonoid unit structure of each tannin and particularly on the level of colloidal state of the tannin solution and the number-average degree of polymerization (DP_n), with the latter two parameters being the main determining ones for the second reaction step and the first two for the first reaction step. It is, however, the combination of the three parameters that determines the total observable effect for each of the flavonoid tannins. The SiO_2 attack at the heterocycle ether oxygen is of such an intensity that the A-rings' phenoxide radicals, which drive the reaction, surge very rapidly to such a higher proportion than the B-rings phenoxide radicals that the B-rings also start to surge later by shifting to the left of the $^{\bullet}B \rightleftharpoons A^{\bullet}$ equilibrium. There are also indications that ionic mechanisms might be more important for the second step of the reaction. Different radical-anion species and the relative movements of the relevant equilibria involved can be clearly identified from the spectra peaks. The initial, maximum intensity of the peaks has been shown to be the parameter defining the first step of the reaction, while the radical decay rate has been shown to refer to the second step of the reaction. Hydrolyzable tannins have been shown not to undergo neither any silica-induced radical surge nor autocondensation as predictable from their structures. J Appl Polym Sci **64:** 243–265, 1997

Key words: tannins; flavonoids; autocondensation; radical reactions; kinetics; polyflavonoids; polycondensation; structure

INTRODUCTION

Recently, the autocondensation to hardened resins of polyflavonoid tannins induced by weak Lewis acids, in particular silica and silicic acid, has been described.[1–9] Both ionic and radical mechanisms have been found to exist for this reaction for all polyflavonoid tannins.[1,5,6,8] The relative balance in their contribution to the hardening of the two types of mechanism differs according to the type of tannin used, hence, with the difference

Correspondence to: A. Pizzi.
 CCC 0021-8995/97/020243-23

in structure of the tannin repeating unit.[5] The differences in the kinetics of the reaction depending on the structure of the tannin can be investigated according to two different approaches. In the previous article,[6] it was investigated for one type of tannin only, treated according to different procedures to induce known modifications to its structure and to the colloidal state and behavior of its solutions. In this article instead, the kinetics of induced radical autocondensation of different types of tannins of different, but well-known structures are investigated.

The polyflavonoid tannins in industrial tannin extracts are composed mainly of flavan-3-ols repeating units. Four types of repeating units can exist and predominate in these tannins,[10] as follows:

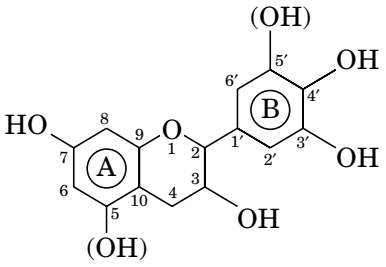

Polymers in which the flavonoid unit A and B rings both present the extra —OH group are called prodelphinidins; only the extra —OH on the A ring are called procyanidins, only the extra —OH on the B ring are called prorobinetinidins, and none of the extra —OHs are called profisetinidins.[11] Such differences in structure, although they appear to be minor, induce instead rather well-defined and marked characteristic behavior to the tannin.

Six commercial tannin extracts, each predominantly belonging to one of the four classes described above, were then used. Thus, Pecan (*Carya illinoensis*) nut pith tannin extract, a prodelphinidin tannin (prodelphinidins: procyanidins structures = 6 : 1), Pine (*Pinus radiata*) bark tannin extract (an entirely procyanidin tannin of high DP_n), Quebracho (*Schinopsis balansae,* variety chaqueno) wood tannin extract (a predominantly profisetinidin/prorobinetinidin tannin), Mimosa (*Acacia mearnsii,* formerly *mollissima,* de Wildt), cube Gambier (*Uncaria gambir*) shoots tannin extract (an entirely procyanidin tannin of low DP), and Sumach (*Rhus coraria*) tannin extract were used.

To ascertain that the effect described was characteristic of flavonoid tannins, the experiment was also repeated with three hydrolyzable tannins. The model compound (+)-Catechin, a monomeric flavonoid of structure of type (II) was also investigated under the same reaction conditions.

EXPERIMENTAL

Tannin Types

The following six types of commercial polyflavonoid tannin extracts were used.

- Natural Quebracho (*Schinopsis balansae,* variety chaqueno) wood tannin extract, from Indunor, Argentina.
- Pecan (*Carya illinoensis*) nut pith tannin extract, courtesy of Advanced Resin Systems, Memphis, U.S.A., and of Bakelite AG, Duisburg, Germany.
- Pine (*Pinus radiata*) bark tannin extract from Diteco Ltda., Chile.
- Mimosa (*Acacia mearnsii,* formerly *mollissima,* de Wildt) bark tannin extract (ex Brazil) from Silva-Ledoga, Italy.
- Gambier (*Uncaria gambir*) shoots tannin extract (ex Indonesia), from Silva-Ledoga, Italy.
- Sumach (*Rhus coraria*) tannin extract, from Silva-Ledoga, Italy.

Three types of commercial hydrolyzable tannin extracts were used for control: namely, Chestnut (*Castanea sativa*) wood tannin extract (ex Silva-Ledoga, Italy), Oak (*Quercus robur*) bark tannin extract (ex Isoroy, France), and Tara (*Caesalpina spinosa*) tannin extract (ex Silva-Ledoga, Italy).

Tannin Extract Solutions

Tannin extract water solutions of 20% concentration were prepared by dissolving spray-dried powders (except for gambier and oak, for which finely ground tannin extract powders were used) of the different types of tannin extracts in water and adjusting the water pH to 12 with 30% sodium hydroxide solution, to which 10% SiO_2 on tannin extract solids was or was not added. Solutions of 5% (+)-catechin monomer at the same pH were used as a control.

Electron Spin Resonance (ESR) Spectra

ESR spectra of the above solutions without and with 10% fine SiO_2 powder (aerosyl) were done. ESR spectra were recorded at 298 K on a Bruker ER 200 D spectrometer (X-band) equipped with TE_{102} sample cavity. Fine structures of the phenoxide radicals were studied in the range of 3465–3495 gauss with field modulation intensity of 0.8 and scan times of 500 s. The spectra in air, due to the requirement of the presence of singlet oxygen for the radical mechanism of pyran ring opening to occur,[5,12] are the ones reported. The tannin phenoxide signals were observed at 3482.4 gauss, and all had g = 2.003. Spectra were centered on the signal of DPPH as standard[13] at 3843 gauss. Decay of the radical concentration, of the variation in intensity of the peaks of the fine structure of the phenoxide signal as a function of time, were followed by scanning the material after alkali addition, or both alkali and silica addition at five minute interval for a period of 1 h or more. The first-order kinetic equations of the second step of the reaction, namely, the radical decay reaction, were expressed as signal intensity units (r) in function of time. Pine could not be modelled in a consistant manner, while pecan and catechin monomer responded to kinetic equations both different and more complex than the other tannins. For this reason, and to present comparable reaction half times and rates of radical decay, all the tannins and the model compounds were also modelled by a Bezier polynomial[14]; these values are also reported in Table I and form the base for comparisons of all the materials in regard to half reaction times. Maximum intensities reported are the experimental values. The rates of the radical decay reaction in Table II were obtained by dividing the rate of the same reaction expressed in signal intensity units per second^{-1}, by the maximum intensity of the signal; their unit is then s^{-1}, and they have the magnitude of a first-order rate constant.

RESULTS

1. For all the tannins studied that are in colloidal state,[2,6,15–18,26–28] peak intensity, hence, radical concentration (Table I), increases considerably when SiO_2 is present, with the exception of mimosa tannin (and of catechin, which is not colloidal in solution).
2. For all the tannins studied that are in colloidal state,[2,6,15–18] the reaction half-time becomes shorter (Table II); hence, the radical decay rate and the rate of tannin autocondensation are more rapid when SiO_2 is added (with the exception of sumach extract, in which the presence of a majority of hydrolyzable tannins possibly masks the result of the flavonoid fraction of the extract).
3. Radical concentration as expressed by the peak intensity (Table I) does not appear to be related to radical decay rate (represented by reaction half-time; Table I) as to greater signal intensities correspond both slower and faster radical decay rates (Table I).
4. There appears to be some kind of relationship between the colloidal state of the tannin solution as already determined by other techniques[2,6,15–18] and both the signal intensity, as well as the reaction half-time (Table I).
5. There appears to be some relationship between the predominant structure of the flavonoid unit in the tannin with the radical decay rate (Tables I and II). A similar relationship with the signal intensity appears to exist, but it is less clear.
6. The values of DP_n of each type of tannin determined by ^{13}C NMR[19] and by other techniques[20] appear in most cases to be inversely proportional to the increase of radical decay rate induced by addition of SiO_2 (the lower the DP_n, the more marked is the acceleration of the radical decay rate induced by SiO_2; see Table II).
7. The value of the DP_n appears to have the more marked influence on the radical decay rate (both in presence or absence of SiO_2), while the colloidal state appears to be the second most important factor.

DISCUSSION

The results of the comparative kinetics of radical concentration decay for all the different types of polyflavonoid tannin extracts are shown in Table I and show several features of interest. Firstly, the intensity of the ESR signal, hence, the radical concentration at parity of tannin concentration, does not appear to be related to the rate of radical decay. In short, the rates of radical formation and radical decay appear in the main to be unrelated,

Table I Kinetic Laws, Peak Intensities and Reaction Half-times of Alkali and Silica-induced Tannins Autocondensation

Alkali Alone (pH = 12)						Alkali (pH = 12) + 10% SiO_2					
Peak (Gauss)	Ring	Kinetic Law	Reaction Half-time (s)		Peak Intensity at $t = 0$ ($\times 10^{-5}$)	Peak (Gauss)	Kinetic Law	Reaction Half-time (s)		Peak Intensity at $t = 0$ ($\times 10^{5}$)	Ratio
Quebracho											
3476.9	A	$r = 98.3680\ e^{-0.1168t}$	356	457	115.92	3477.9	$r = 411.1190\ e^{-0.1392t}$	299	312	454.68	3.9
3479.0	B	$r = 75.1567\ e^{-0.1223t}$	340	370	66.97	3478.9	$r = 502.0077\ e^{-0.1354t}$	307	326	523.36	6.6
3480.7	B	$r = 110.8841\ e^{-0.1287t}$	323	435	134.52	3480.4	$r = 531.9474\ e^{-0.1279t}$	325	366	576.28	4.3
3482.9	A	$r = 126.4532\ e^{-0.1361t}$	305	410	153.02	3482.9	$r = 310.8174\ e^{-0.1082t}$	384	454	347.24	2.3
Average				418	120	Average			364	475	
Mimosa											
3477.6	A	$r = 7059.45\ e^{-0.4200t}$	99	113	6855.6	3477.8	$r = 5925.21\ e^{-0.7058t}$	59	70	5856.6	0.9
3478.3	A	$r = 9145.46\ e^{-0.3499t}$	119	116	8267.3	3478.6	$r = 7628.81\ e^{-0.6876t}$	61	71	7503.6	0.9
3479.3	A	$r = 4672.08\ e^{-0.4155t}$	100	117	4577.6	3479.5	$r = 4247.38\ e^{-0.7096t}$	59	71	4225.4	0.9
3480.3	B	$r = 6402.63\ e^{-0.4215t}$	99	118	6291.7	3480.5	$r = 5747.45\ e^{-0.7177t}$	58	70	5710.8	0.9
3481.2	B	$r = 9911.95\ e^{-0.3841t}$	108	120	9407.2	3481.4	$r = 8991.96\ e^{-0.6905t}$	60	71	8842.7	0.9
3482.2	B	$r = 4204.06\ e^{-0.3286t}$	127	125	3703.5	3482.4	$r = 4095.23\ e^{-0.6157t}$	68	69	3757.0	1.0
3482.9	B	$r = 8296.04\ e^{-0.3566t}$	117	129	8443.1	3483.1	$r = 7982.22\ e^{-0.6431t}$	65	79	7928.9	0.9
3483.8	A	$r = 6600.28\ e^{-0.4038t}$	103	122	6495.3	3484.0	$r = 5825.70\ e^{-0.6611t}$	63	75	5788.9	0.9
3485.7	A	$r = 7418.12\ e^{-0.4145t}$	100	119	7271.6	3485.9	$r = 6511.80\ e^{-0.6960t}$	60	71	6458.2	0.9
3486.5	A	$r = 7434.80\ e^{-0.4254t}$	98	114	7235.6	3486.6	$r = 6180.75\ e^{-0.7372t}$	56	67	6128.4	0.9
Average				119	6850	Average			71	6220	
Sumach											
3480.4	A	$r = 93.8401\ e^{-0.9587t}$	43	45	96.12	3480.8	$r = 136.4779\ e^{-0.8629t}$	48	51	141.9	1.5
3481.4	A	$r = 189.8409\ e^{-0.8836t}$	47	49	194.35	3481.7	$r = 238.5303\ e^{-0.7937t}$	56	58	244.8	1.3
3482.4	B	$r = 102.1278\ e^{-0.9045t}$	46	47	102.94	3482.6	$r = 120.5295\ e^{-0.4691t}$	89	87	118.9	1.2
3482.9	B	$r = 363.4073\ e^{-0.8362t}$	50	51	370.23	3483.2	$r = 480.7769\ e^{-0.6416t}$	65	66	487.3	1.3
3483.8	A	$r = 150.5243\ e^{-0.7553t}$	55	57	154.70	3483.9	$r = 170.5689\ e^{-0.5067t}$	82	85	174.5	1.1
3484.4	A	$r = 113.3997\ e^{-0.9418t}$	44	45	114.98	3484.6	$r = 207.7799\ e^{-0.7132t}$	58	60	210.5	1.8
Average				49	172	Average			67	229	

Table I (*Continued*)

Alkali Alone (pH = 12)								Alkali (pH = 12) + 10% SiO_2								
				Reaction Half-time		Peak Intensity at $t = 0$					Reaction Half-time		Peak Intensity at $t = 0$			
Peak (Gauss)	Ring	Kinetic Law		(s)	(s)	($\times 10^{-5}$)		Peak (Gauss)	Kinetic Law		(s)	(s)	($\times 10^{5}$)		Ratio	
Pine																
3479.7	A	—		—	341	489.96		3478.9	—		—	156	898.58		1.8	
3480.9	A	—		—	202	476.45		3480.0	—		—	156	875.65		1.8	
3481.9	B	—		—	133	390.60		3480.8	—		—	125	836.34		2.1	
3482.4	B	—		—	160	345.84		3481.6	—		—	131	599.14		1.7	
3483.4	A	—		—	615	444.92		3482.4	—		—	185	885.75		2.0	
3484.6	A	—		—	842	449.79		3483.6	—		—	172	1044.33		2.1	
Average					381	441		Average				154	856			
Pecan																
3479.6	A	—		—	4215	366.72		3479.7	—		—	149	922.32		2.5	
3480.7	B	—		—	310	379.41		3480.6	—		—	135	1059.08		2.8	
3483.3	B	—		—	1820	388.96		3483.3	—		—	160	898.58		2.3	
3484.4	A	—		—	310	602.92		3484.5	—		—	135	1584.52		2.6	
Average					1663	434		Average				144	1115			
Gambier																
3480.4	A	$97.6225\ e^{-0.1390t}$		299	1687	186.26		3480.5	$133.548\ e^{-0.1276t}$		326	961	203.63		1.1	
3481.6	B	$75.8529\ e^{-0.0906t}$		459	4807	147.09		3481.7	$73.4932\ e^{-0.0570t}$		251	2993	128.77		0.9	
3483.5	B	$149.508\ e^{-0.0584t}$		712	1012	179.84		3483.6	$152.013\ e^{-0.0584t}$		712	1392	203.25		1.1	
3484.7	A	$100.191\ e^{-0.2148t}$		194	—	211.00		3484.8	$185.460\ e^{-0.1275t}$		326	635	249.01		1.2	
Average				416	2502	181		Average			404	1495	196			
Catechin Monomer $r = (c - b)/(1 + e^{d(t-a)})$																
		a	b	c	d				a	b	c	d				
3480.5	A	8.29	0.00	17.56	0.42	—	488	16.91	3480.8	2.92	0.00	10.50	1.56	—	174	11.84	0.70
3481.0	A	8.05	0.82	34.40	0.62	—	472	34.61	3481.2	3.03	0.00	21.56	1.51	—	181	22.44	0.65
3481.5	A	8.00	0.10	56.36	0.57	—	477	55.32	3481.7	2.94	0.00	34.03	1.80	—	176	36.33	0.66
3482.2	B	7.86	0.00	44.31	0.60	—	470	44.29	3482.4	2.85	0.00	26.84	1.81	—	171	29.27	0.66
3482.6	B	7.99	1.90	51.85	0.66	—	464	53.41	3482.9	2.81	0.00	31.96	1.59	—	168	34.55	0.63
3483.1	B	7.67	0.02	55.23	0.60	—	458	56.59	3483.4	2.80	0.00	33.63	1.60	—	167	37.47	0.66
3483.6	A	7.67	0.00	63.40	0.56	—	457	64.17	3483.9	2.76	0.00	38.56	1.41	—	164	42.81	0.67
3484.3	A	7.98	0.12	44.87	0.57	—	476	44.99	3484.6	2.72	0.00	26.48	1.79	—	163	30.18	0.67
3484.9	A	7.73	2.01	70.09	0.67	—	452	71.13	3485.1	2.72	0.00	43.50	1.54	—	162	46.07	0.65
Average							468	49	Average						169	32	

Table II Reaction Rates of the Radical Decay Reaction (Second Reaction Step), Rate Ratios, and Number-average Degree of Polymerization (DP_n) for Different Tanins and Catechin Model

Tannin Type	Reaction Rate Without Silica (s^{-1})	With Silica	Rate Ratio	DP_n[19,20]
Mimosa	4.37×10^{-3}	7.35×10^{-3}	1.68	4.9
Pine	4.54×10^{-3}	6.04×10^{-3}	1.33	5.9
Pecan	3.88×10^{-3}	5.23×10^{-3}	1.35	5.5
Quebracho	1.81×10^{-3}	2.04×10^{-3}	1.13	6.7
Gambier	0.74×10^{-3}	0.68×10^{-3}	0.92	1.7
Sumach	13.9×10^{-3}	10.8×10^{-3}	0.78	—
Catechin monomer	0.09×10^{-3}	0.27×10^{-3}	3.00	1.0

in the presence or absence of SiO_2; the intensity of the signal is directly related to the rate of radical formation, hence, to the first reaction step of tannin autocondensation[1,6,8] which is the flavonoid pyran ring opening; while the rate of radical decay appears to be directly related to the second reaction step, hence, to the condensation step proper of the reactive site formed on a flavonoid unit with another flavonoid unit.[1,6,8]

The pattern of ESR signal intensities and radical rates of decay (Table I) can then be interpreted as the observable combination of two consecutive reaction steps, namely,

$$\underset{\text{unit}}{\text{Flavonoid}} \xrightarrow[\text{pyran ring opening}]{\text{radical formation}} \underset{\text{radical-anions}}{\text{Flavonoid unit}} \xrightarrow{\text{condensation}} \underset{\text{products}}{\text{Cross-linked}}$$

It is the predominance of one of these two reaction steps that will determine the behavior of the tannin; or better, it is the structure of the main type of flavonoid unit in each tannin that will determine to what extent each reaction step is the rate-determining one. In this context, it is necessary to discuss the behavior of the different tannins, at first, in the case of SiO_2 being absent. Without SiO_2, it is quite evident from Table I that by the value of the maximum peak intensity (= radical concentration induced in the system), Mimosa tannin presents a radical concentration far higher than the other tannins. It also presents a half-time of reaction that is the second shortest; although, in this case, the difference with the other tannins is not as great as for the signal intensity. It is quite evident for Mimosa tannin, then, that the second reaction step is the rate-determining one. This is the consequence of a faster first step due to the main prorobinetinidin structure[21,22] of mimosa being well-known for facile opening at the heterocycle pyran ring.[10,23] It is also a consequence of the relative slowness of the subsequent condensation due to the resorcinol-type A-rings of the more abundant flavonoid unit of Mimosa extract.[23,24] The total observable effect will then be a rapid increase in radical concentration, practically throughout the majority of the robinetinidin units of this tannin, hence, a very high signal intensity due to the following reaction step being relatively slower than the first one.

For the other tannins, the situation is very similar if the differences in their structures are also taken into consideration. Their structures are less prone to facile heterocycle opening in absence of silica[1,10,23]; hence, their first reaction step is slower and less extensive and, as a consequence, their signal intensities are much lower than for Mimosa tannin. The follow-up reaction for pine and pecan tannins has a rate very similar to that of mimosa tannin (Table II), in relation to original radical concentration. Quebracho tannin has an even slower rate of autocondensation (as shown already by other techniques[1,7,8]) but also shows that it has a slower rate for the first reaction step (low signal intensity). This confirms that quebracho profisetinidins have a much lower tendency than mimosa prorobinetinidins to open at the pyran heterocycle. This effect, the effect of the difference in influence of catechol- and pyrogallol-type B-rings on heterocycle opening[1,10,23] is also evident, although to a much lesser extent, for the differences between pine and pecan tannin (Table I).

It is interesting to see what happens on addition of SiO_2 to the tannin solutions. For mimosa tannin, the increase in the rate of the second reaction step is greater than for the first reaction step. This is due to the fact that most of the main robinetinidin units of mimosa (as much as 80% of tannin repeating units[21,22] open at the heterocycle

even without the help of SiO_2; thus, there is not much more room left to maneuver to increase the rate of the first reaction step (and not many main units remain still unopen). The net consequence is that the radical concentration, while still remaining high, becomes approximately 10% lower than in the case of SiO_2 being absent.

For pine and pecan tannins (a procyanidin, the first one, and mainly a prodelphinidin, the second one) instead, the majority of flavonoid units are still available for opening of the heterocycle. Addition of SiO_2, by inducing such an opening, then increases the reaction rate for the first step (by simply increasing the proportion of open units) to a greater extent than the rate for the second reaction step. As a consequence, the signal intensities increase as there is an increased concentration of radicals at the intermediate stage of the total reaction.

Quebracho tannin presents a similar behavior pattern to pecan and pine, with a marked increase in signal intensity but with the sole difference that the rate of the second reaction step is only slightly increased. For Gambier tannin ($DP_n = 1.73$),[19] which has much lower DP_n than the other tannins,[19,20] as it is composed of approximately 50% monomeric catechin, addition of SiO_2 only increases very slightly the signal intensity and does not the radical decay rate at all. Sumach tannin presents a mild increase in signal intensity and a decrease in the rate of the subsequent radical decay. Lastly, catechin monomer shows a slight decrease in signal intensity and an increase in radical decay rate (although starting from a very low value).

The characteristic behavior of each tannin can be related to their differences in structure, to the presence or no presence of other reactions, and to the colloidal level of the solutions. Thus, mimosa tannin (mainly a prorobinetinidin, but with noticeable proportions of profisetinidins[21,22]) shows the characteristic ease of pyran ring opening of prorobinetinidins, and all reactions are dominated from this characteristic.

Pine and pecan tannins (procyanidin and prodelphinidin) present a greater difficulty of pyran ring opening than mimosa, but on addition of the SiO_2 catalyst, prodelphinidins show that heterocycle opening is easier in their case than for procyanidins (as determined already by other techniques[1,10,23]), but never to the same extent of mimosa prorobinetinidins. Quebracho profisetinidins present the same difficulty in opening the heterocycle as pine procyanidins, confirming that, in both cases, the predominance of catechol B-rings depresses, in absence of SiO_2, heterocycle opening in favor of interflavonoid bond cleavage (a well-documented occurrence in procyanidins,[1,25] but only recently ascertained for profisetinidins[10,19,23]). While in procyanidins and in prodelphinidins the high reactivity of the A-ring which drives the second step of the reaction then increases the rate of the radical decay reaction, the lower reactivity of the A-ring of quebracho profisetinidins does not allow this; hence, the increase in rate of the follow-up reaction when SiO_2 is added is less noticeable. In gambier tannin (a procyanidin), which is composed of up to 50% of monomeric catechin, its low DP_n ($DP_n = 1.73$)[19,20] conjures that the depolymerization that takes place by interflavonoid bond cleavage assumes greater relative importance. The net effect is an apparent increase in signal intensity, which is less marked, as well as an unchanged rate for the second step of the reaction. A similar side reaction occurs in procyanidins, but their much higher DP_n minimizes its relative importance in pine tannin.

Monomeric catechin shows both lower signal intensity and decay rate than the polymeric tannins. The lower intensity, as well as much slower decay rate, are mainly due to the lack of colloidal state of the solution, as already reported.[2,3,6] Notwithstanding this, the reaction still occurs. This, again, points out that the radical response of these tannin reactions is so intense as a consequence of the colloidal state of their solution.[6] In pecan tannin solutions, the colloidal state of the solution is exclusively due to the tannin[2] for the absence of polymeric carbohydrates[15,26]; this indicates that for pecan tannin solutions, radical response (both concentration of generated radicals as well as radical decay rate) would become more marked than that shown in Tables I and II if polymeric carbohydrates are added: it is particularly the first reaction step that is affected by the colloidal state of the solution.[6] The increase in radical decay rate for the catechin monomer shows that the second step of the reaction is not affected, or is affected to a much lesser extent, by the colloidal state of the solution.

The structure of sumach is less known, although the predominant repeating unit is likely to be fisetinidin[27,28] if one considers the structure of other *Rhus* species.[29] An increase in signal intensity is noticed, but a slowing down of the second step of the reaction is also noticed. It is the only flavonoid tannin among those tested for which the SiO_2 addition causes a signal intensity increase accompanied by a slowing down of the radical decay rate. It might be possible that the

reported presence of some proportion of low reactivity monomeric hydrolyzable tannins, which has been reported,[28] can account for the slowing down of the second step of the reaction.

A point that is of interest to discuss is the relative importance of tannin structure versus colloidal state[2,16–18] of the solution regarding induced radical autocondensation of tannins. There is no doubt that the lack of colloidal state, or a low level of it, greatly affects both the first and the second step of the raction, as shown in the cases of natural and desugared quebracho,[6] and in the case of noncolloidal catechin solutions.[1,3] It is also important to note that even with all the carbohydrates removed, a certain level of colloidal state is imparted to concentrated tannin solutions by the higher molecular weight tannins, as shown for quebracho,[6] and for pecan tannins.[2] This means that the reaction will occur for a polymeric tannin also in absence of carbohydrates, but it will be much slower. Thus, in the case of quebracho tannin, elimination of carbohydrates reduced, with and without SiO_2, respectively, the signal intensity from 122 to 105 (without SiO_2) and from 475 to 181 (with SiO_2); while the radical decay reaction passes from a half-time of 314 to 1469 s (both with SiO_2) as the colloidal state given by the polymeric carbohydrates is completely eliminated.[6]

These results indicate that even maintenance of a low level of colloidal state slows down the first step of the reaction, even quite markedly, if SiO_2 is present. This is even more marked if the solution is not colloidal at all as in the case of catechin monomer. At parity of colloidal level, the influence of the tannin structure is more difficult to gauge: for pine and pecan tannins, the only difference is the B-ring structure, and their colloidal level is not

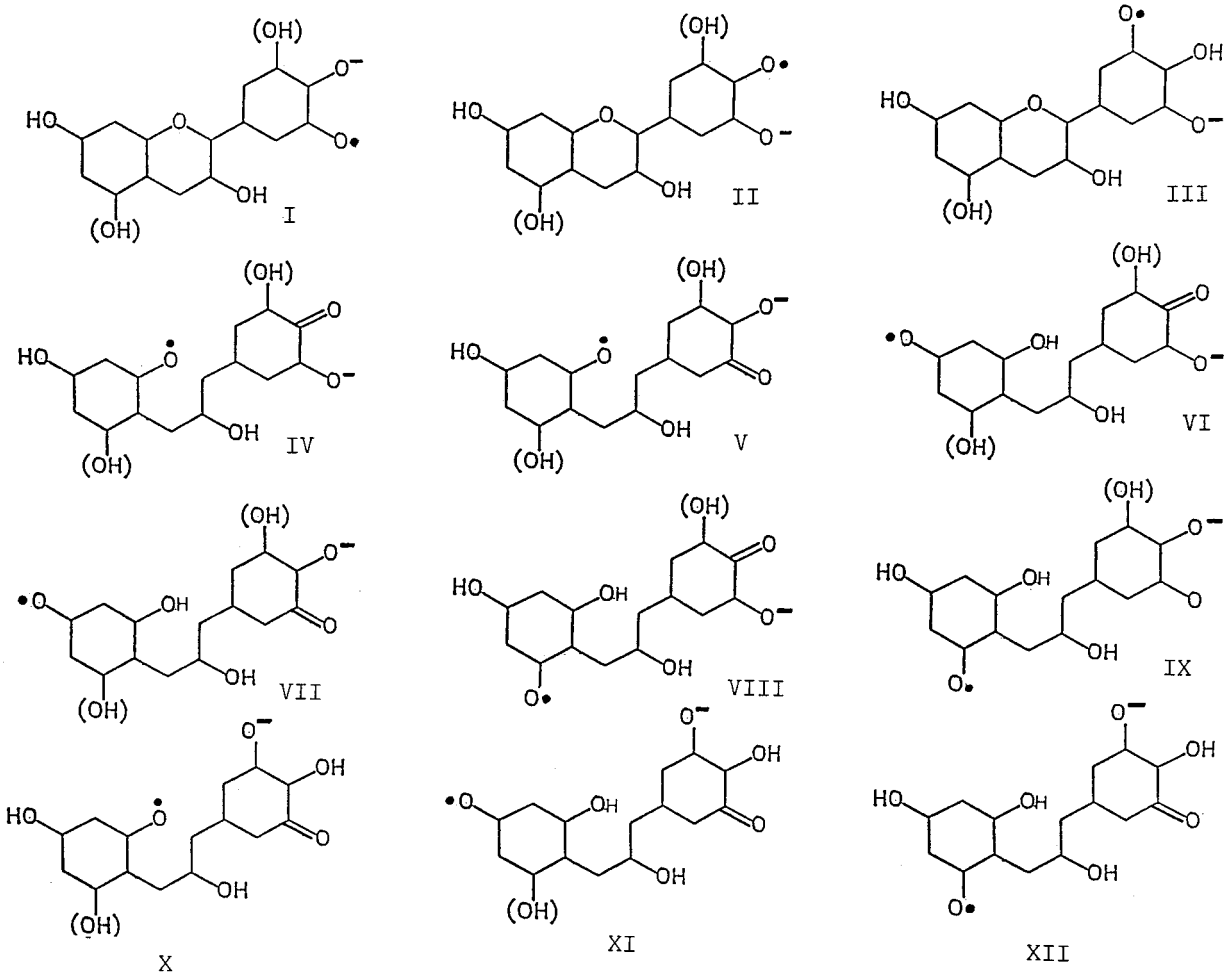

Figure 1 Schematic representation of theoretically possible radical anions of flavonoid units of commercial flavonoid tannins. Only features relevant to the identification of the different radical anions have been reported.

too different.[2] The B-ring difference in structure considerably influences the signal intensity with SiO_2 present, and not at all without SiO_2. It does not influence the radical decay reaction with SiO_2 present, and it does strongly without SiO_2. The picture which then emerges is that at least for the influence of B-ring differences; for the natural tannins, the influence on the first step of the reaction is mild, if at all, while it might be marked for the second reaction step. With SiO_2, small differences in the B-ring structure instead lead to very marked differences for the first reaction step and just about none at all for the radical decay second step.

For A-ring differences (with the exception of mimosa, which has a rather atypical behavior), the first step of the reaction shows marked differences of behavior between phloroglucinol-type and resorcinol-type A-rings (compare pine + pecan with quebracho; Tables I and II) if both SiO_2 is present or absent. For the second reaction step, the influence of structure is clearly evident for all cases (compare pine = pecan ⩾ quebracho; Tables I and II) as would be expected from the higher nucleophilicity of a phloroglucinol A-ring. Thus, in the case of the A-rings, the effect of the structure starts to bear only on the condensation proper (second step) as would be logical to expect.

The colloidal effect, however, appears to be equal to, or much more marked than, the A-ring structure effect for the second reaction step (pine = 381 and pecan = 1663, just on difference of colloidal state imparted by the presence or absence of carbohydrates without SiO_2); The colloidal effect instead appears to be equal or lower than the B-ring structure effect (compare signal intensities with and without SiO_2 for pine and pecan).

It is also of interest to discuss the distribution of the different radical anions that are formed for the different tannin structures. Each peak of the fine structure of the ESR phenoxide radical signal corresponds to a well-defined radical anion or group of radical anions. It is already indicated in Table I what groups of peaks have been found to belong to radical anions in which the radical is on the A- and B-rings of the flavonoid structure. It is also noticeable that different tannins present a different number of peaks and that their intensity varies differently, for different tannins, on addition of SiO_2. All the possible phenoxide radical-anions that could be formed are indicated in Figure 1 (this does not mean that they all form). It is possible to identify which are the radical anions present and their relative proportions, and, hence, to assign to each kinetic laws and behavior, and to ultimately deduce the shifting of the relevant equilibria between different radical-anion species and relate these to the tannin structure. An example based on quebracho tannin will be explained in more detail, and then what was found will be expanded to the other tannins. Quebracho can, in principle, produce six radical anions, each of them in coupled resonance. Thus, radical-anion couples I/II, IV/V, and VI/VII should be detected and give an ESR spectrum composed of three couples of peaks (three downward peaks and three upward ones), with each peak representing a resonance couple of radical anions. The spectrum of quebracho indeed shows this pattern, with two of the peak couples being very well defined (and of which the kinetic laws are presented in Table I) and one less well defined. The radical-anion assignment for each couple of mirror image peaks is shown in Figure 2. In Figures 3–7 are shown the results for all other flavonoid tannins examined and of the catechin monomer.

It is then important to discuss the relative, proportional variation of radical-anion species in each tannin. Without SiO_2, the base-induced mechanism of pyran ring opening already ensures that two-thirds or more of radical anions are with the radical located on an A-ring oxygen. The rate of radical decay is such that the relative proportion of A- and B-ring radicals remains approximately the same throughout the reaction. On addition of SiO_2, the proportion of A-ring radicals increases to more than 85% of the total; in reality, the total amount of both B- and A-ring radicals increases, but the amount of A-ring radicals increases more rapidly, indicating a definite shift towards the right of the equilibrium, as follows,

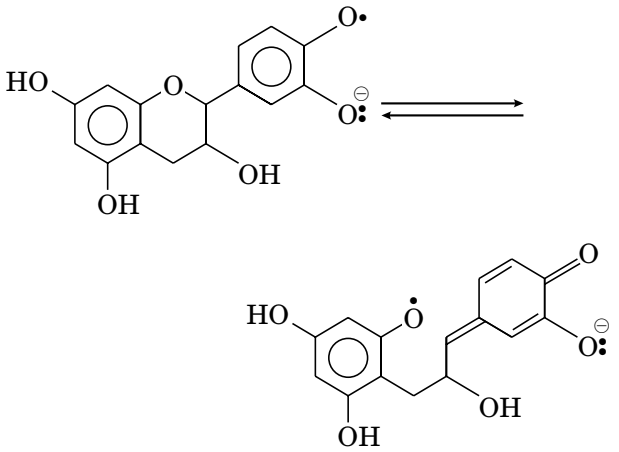

or a reaction independent of the base-induced heterocycle opening, which now is well-known to be

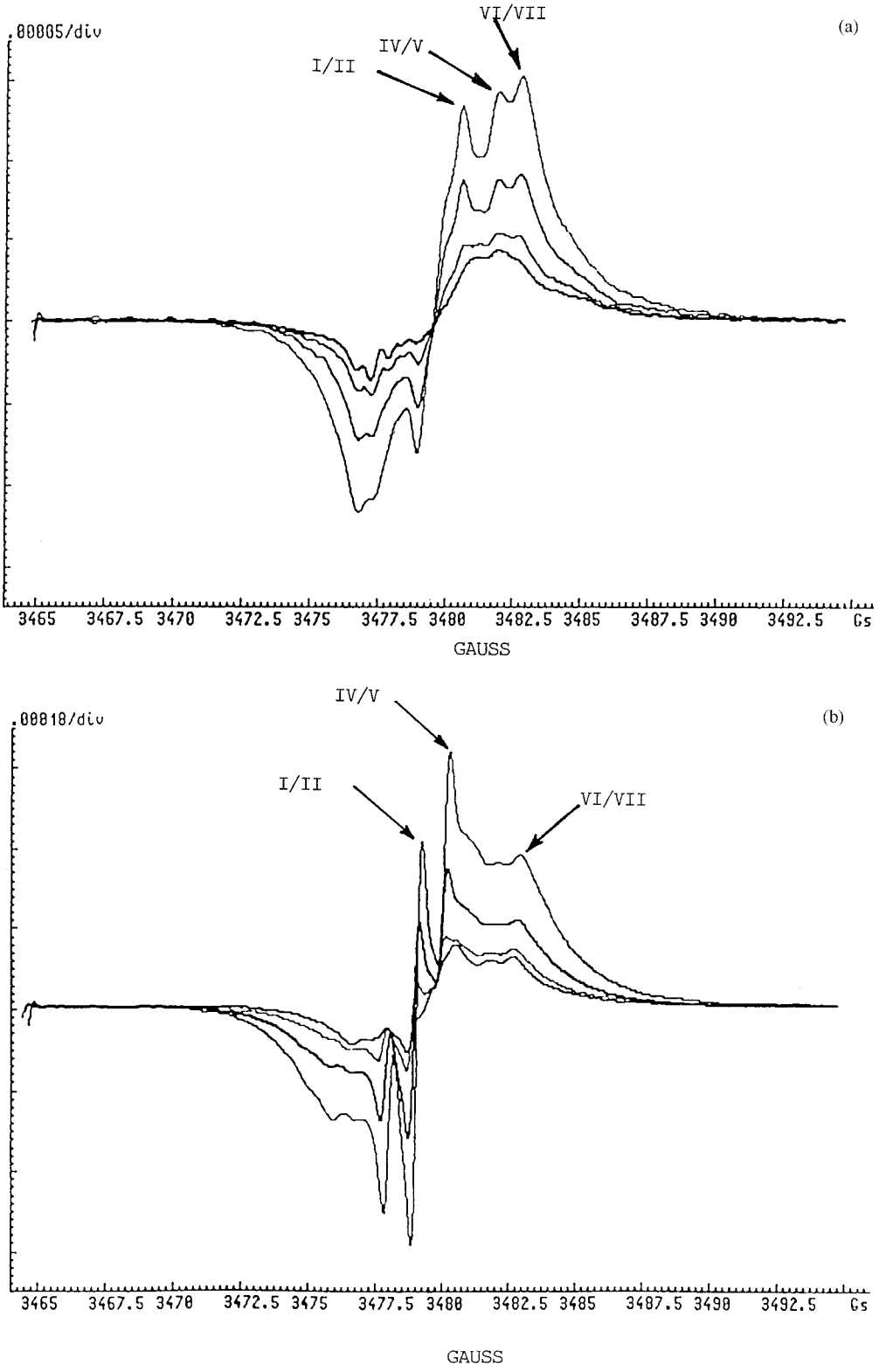

Figure 2 ESR spectra of (a) natural quebracho tannin + base only and (b) quebracho tannin + base + 10% silica at 0 (highest signal intensity), 5, 10, and 15 min after addition of base and base + silica. Peaks corresponding to radical anion couples in resonance are indicated by arrows on the (a) spectrum and the corresponding radical anion couples identified. Note difference between all radical anion peaks between (a) and (b) spectra.

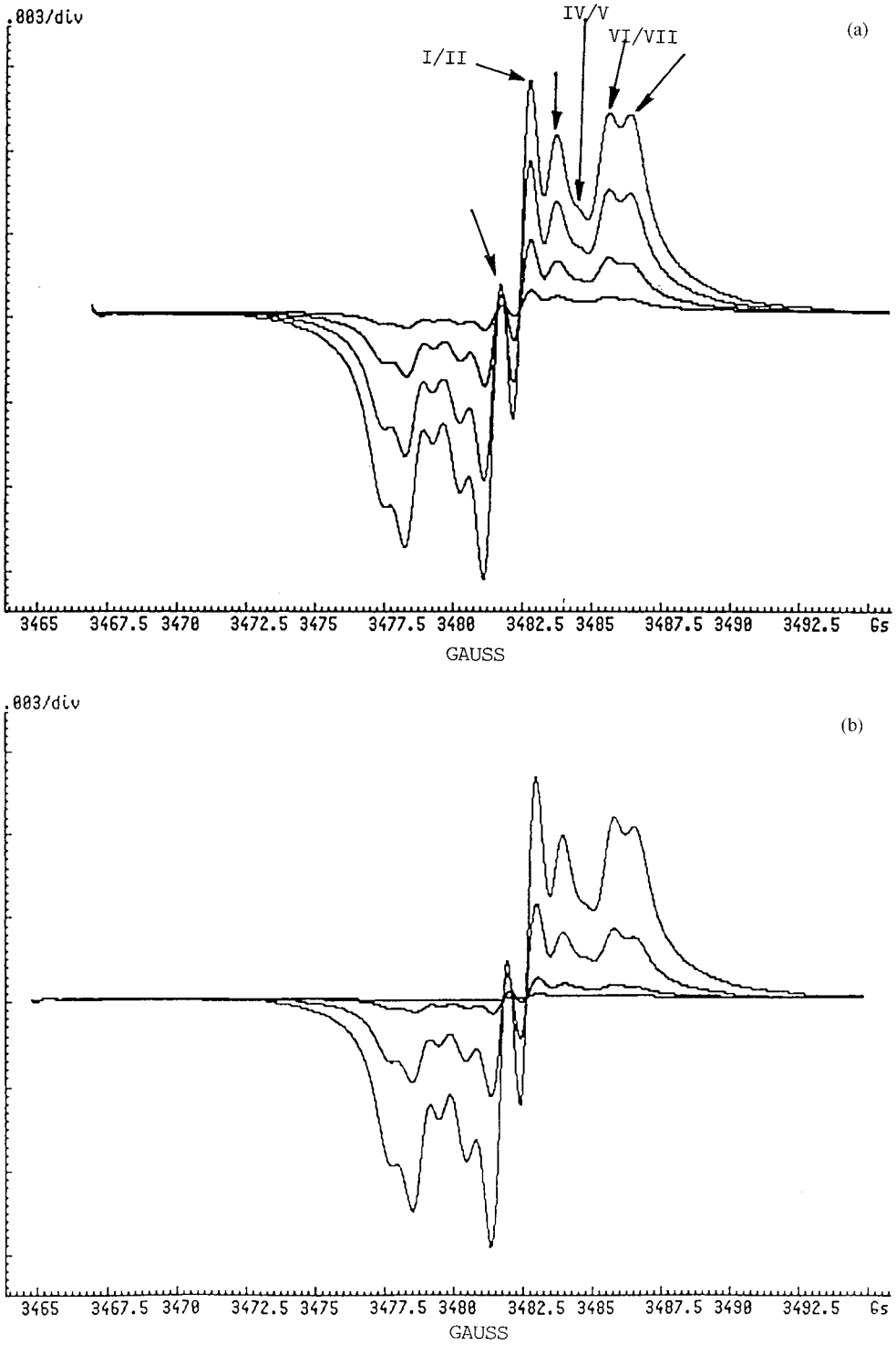

Figure 3 ESR spectra of (a) natural mimosa tannin + base only and (b) mimosa tannin + base + 10% silica at 0 (highest signal intensity), 1.5, 3, and 4.5 minutes after addition of base and base + silica. Peaks corresponding to radical anion couples in resonance are indicated by arrows on the (a) spectrum and the corresponding radical anion couple identified where possible. Note slight difference of the VI/VIII peak between (a) and (b) spectra.

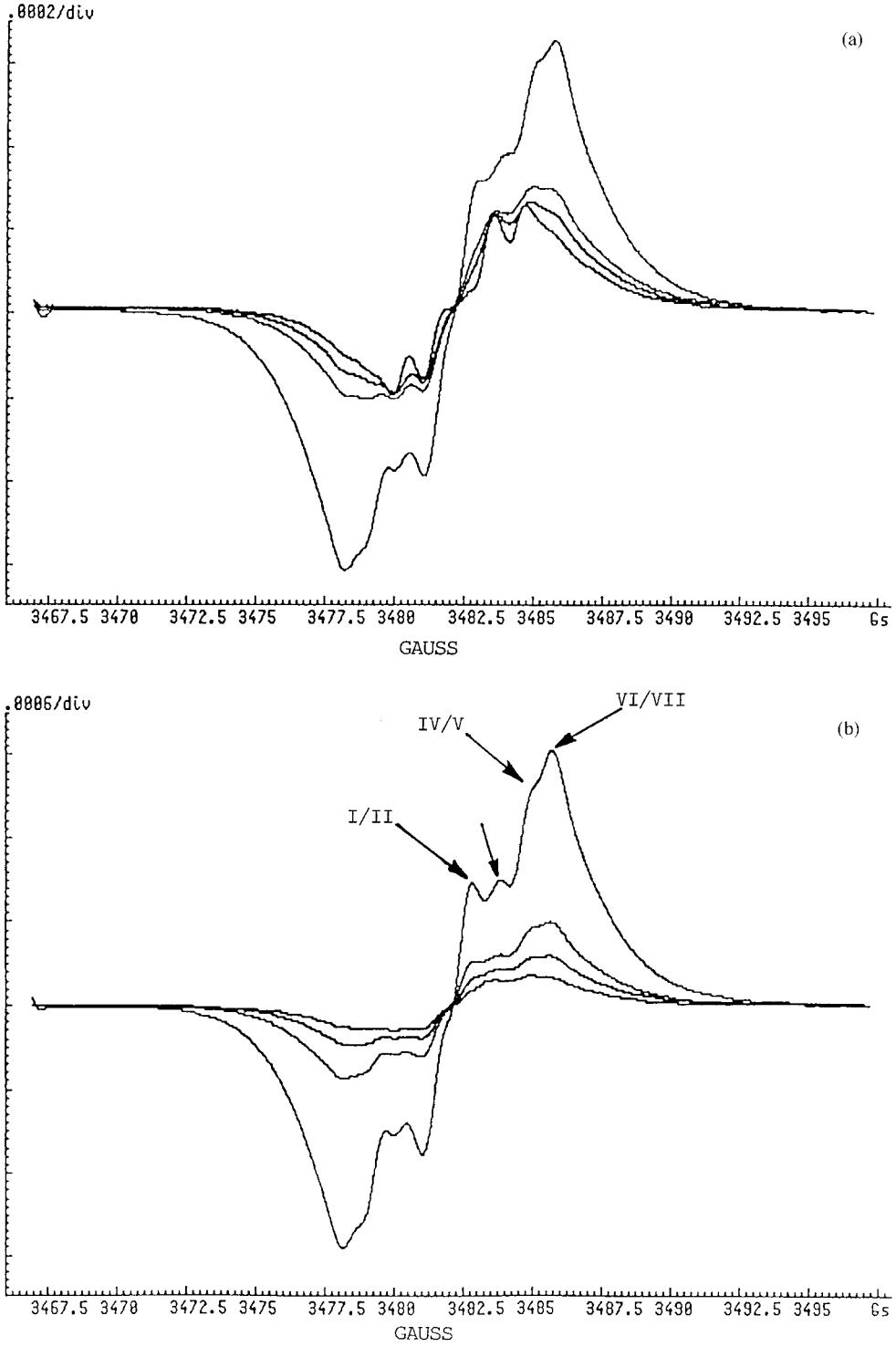

Figure 4 ESR spectra of (a) natural pecan tannin + base only and (b) pecan tannin + base + 10% silica at 0 (highest signal intensity), 2, 3.5, and 6 min after addition of base and base + silica. Peaks corresponding to radical anion couples in resonance are indicated by arrows on the (b) spectrum and the corresponding radical anion couples identified where possible. Note difference of I/II couple between (a) and (b) spectra.

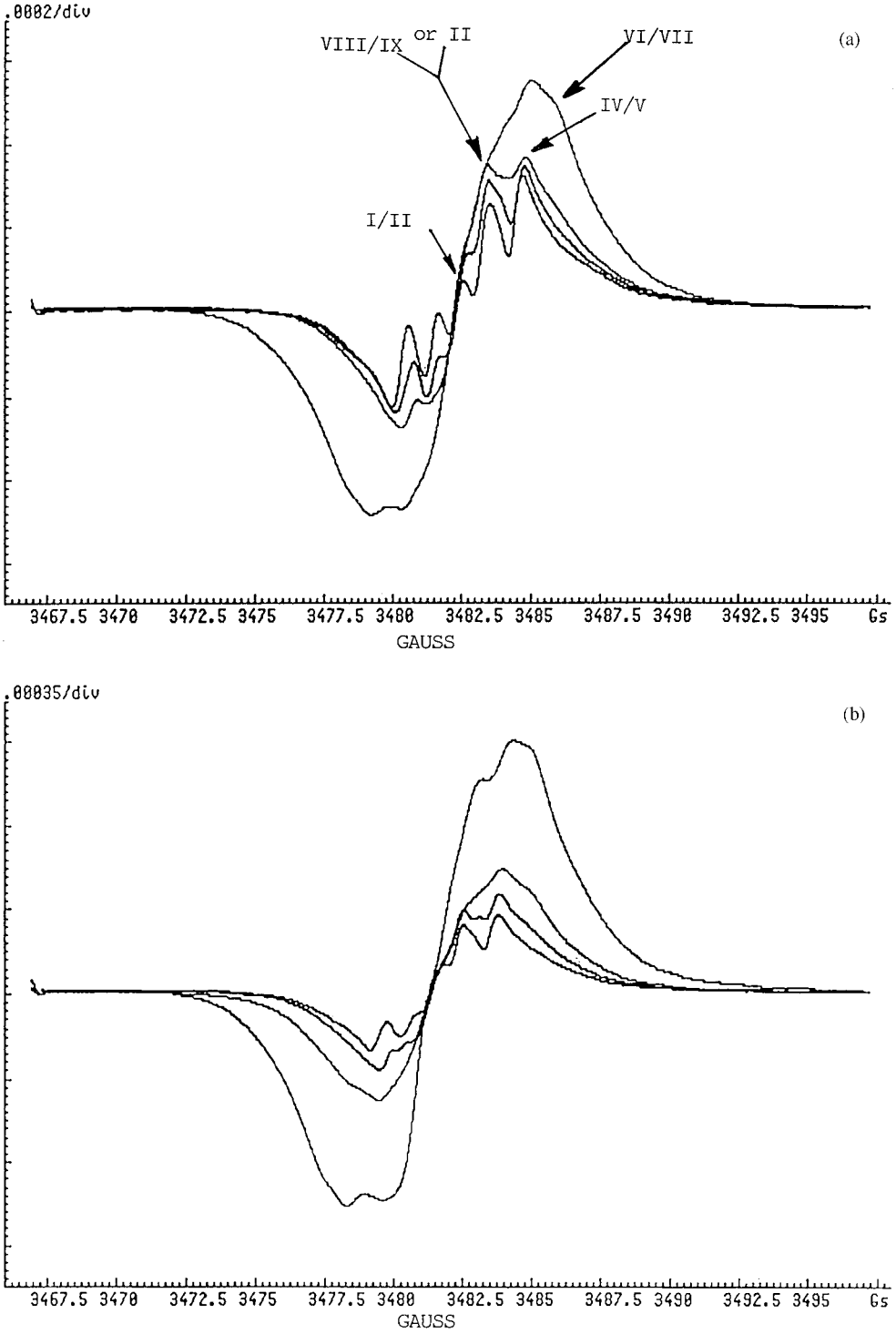

Figure 5 ESR spectra of (a) natural pine tannin + base and (b) pine tannin + base + 10% silica at 0 (highest signal intensity), 1.5, 3, and 6 min after addition of base and base + silica. Peaks corresponding to radical anion couples in resonance are indicated by arrows on the (a) spectrum and the corresponding radical anion couples identified where possible. Note peaks overlap at highest intensity and increasing resolution of bands as the radical decay reaction proceeds.

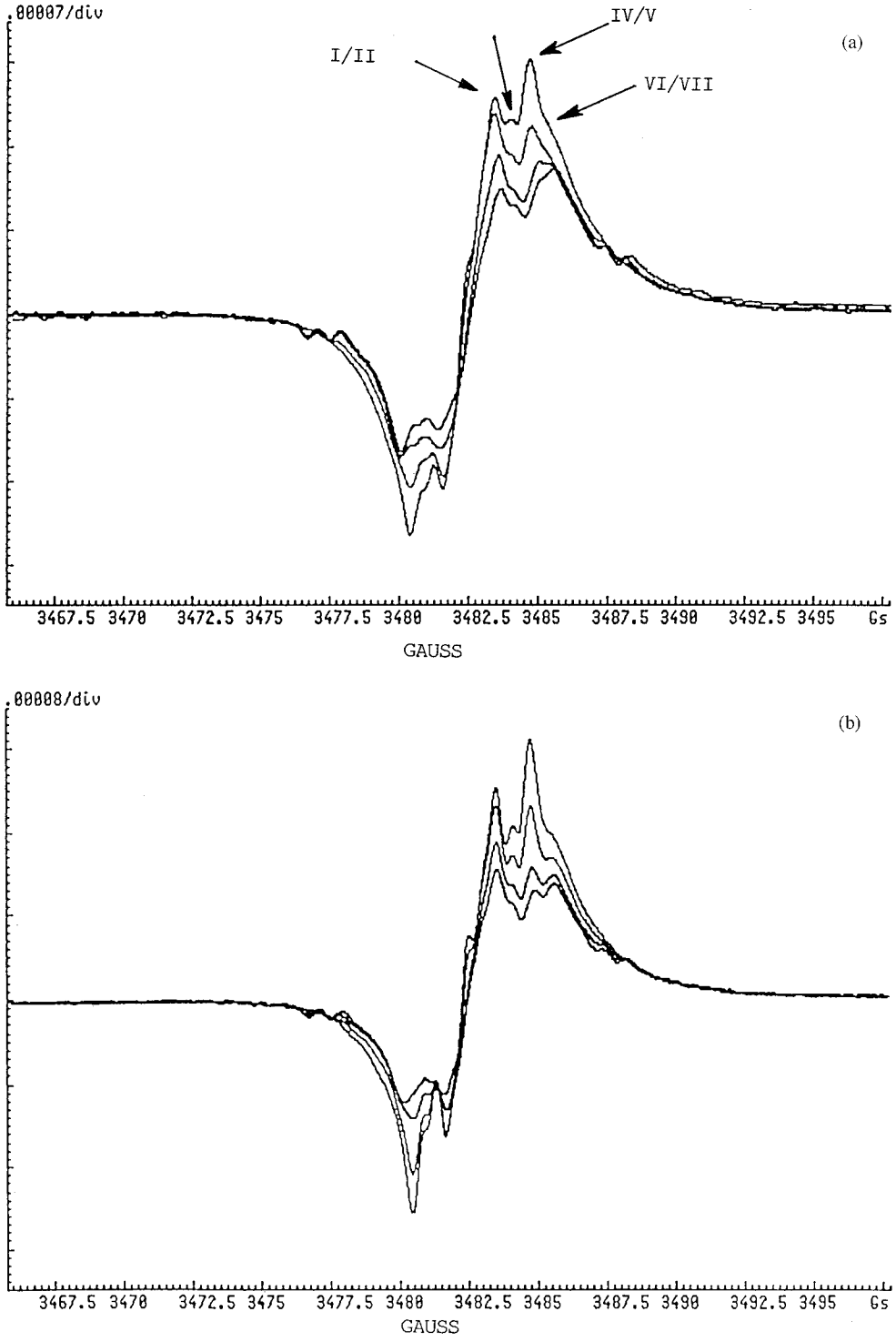

Figure 6 ESR spectra of (a) natural gambier tannin + base only and (b) gambier tannin + base + 10% silica at 0 (highest signal intensity), 3.5, 7.5, and 11.5 min after addition of and of base + silica. Peaks corresponding to radical anion couples in resonance are indicated by arrows on the (a) spectrum and the corresponding radical anion couples identified where possible.

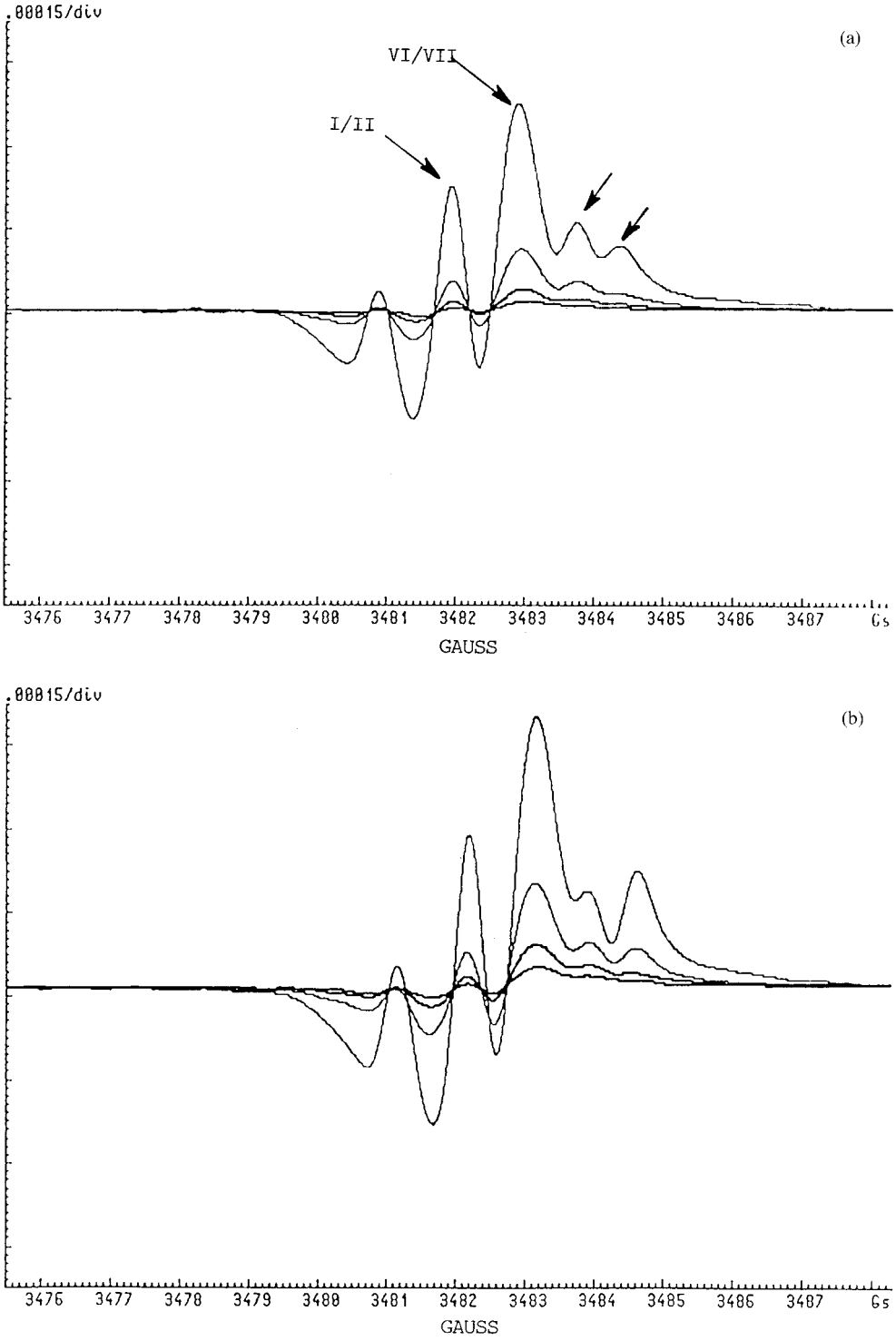

Figure 7 ESR spectra of (a) natural sumach tannin + base and (b) sumach tannin + base + 10% silica at 0 (highest signal intensity), 1.5, 3, and 4.5 min after addition of base or of base + silica. Peaks corresponding to radical anion couples in resonance are indicated by arrows on the (a) spectrum and the corresponding radical anion couples identified where possible.

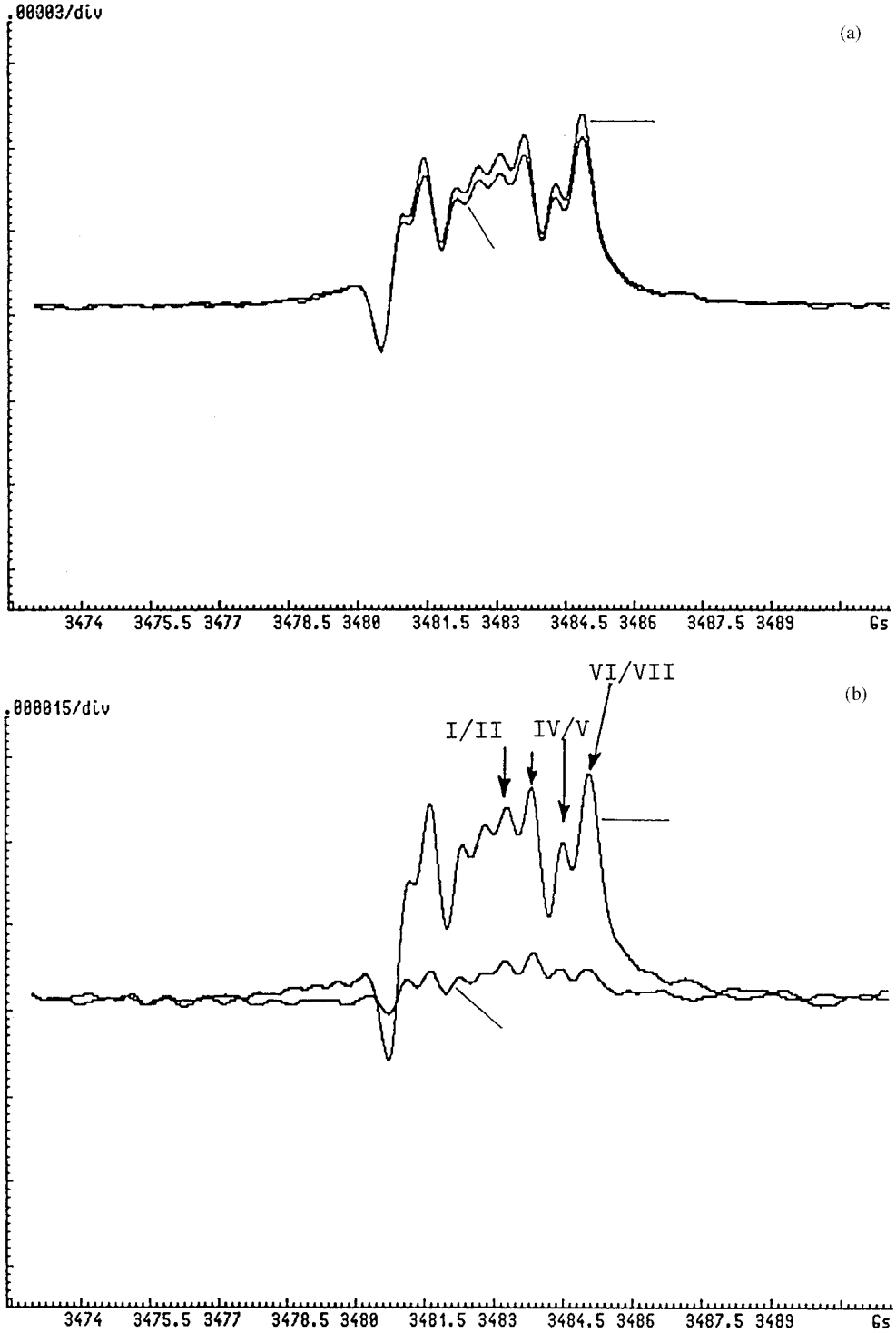

Figure 8 ESR spectra of (a) 5% catechin + base, (b) 5% catechin + base + 10% silica, and (c) 5% catechin + base + 15% silica 5 (highest signal intensity) and 8 min after addition of base or of base + silica. Note much faster radical decay in the cases in which silica is present (difference in intensity between 5 and 8 min curves) and the clear appearance of the characteristic catechinic acid ESR pattern,[31] indicating that the starting compound used was nontypical because it was altered after long storage.

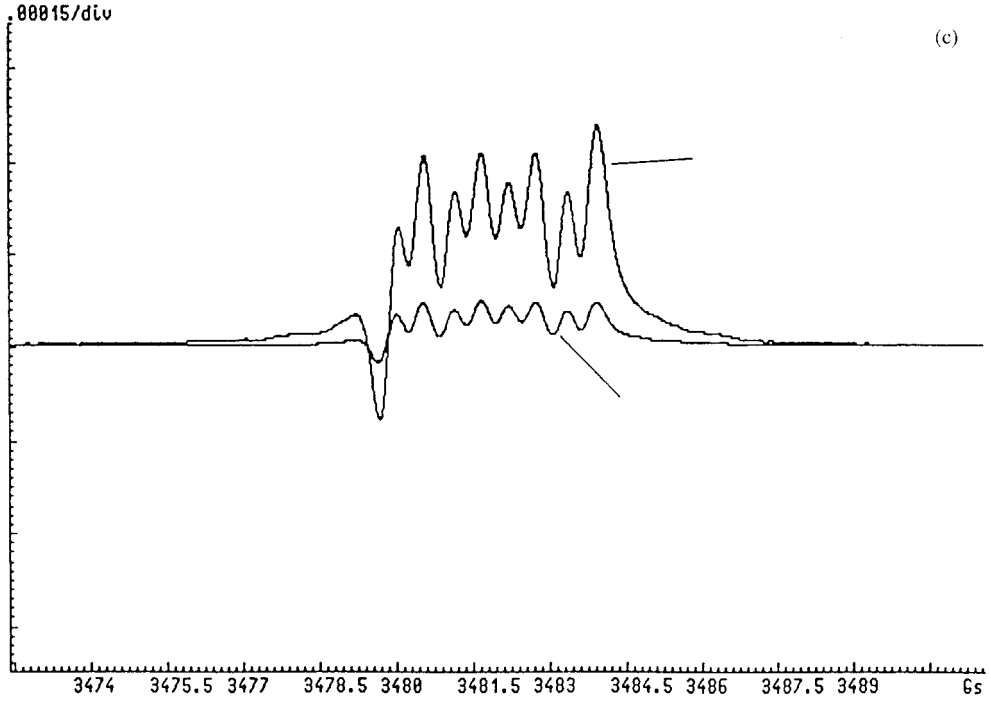

Figure 8 (*Continued from the previous page*)

the direct attack of silicic acid on the heterocycle ring oxygen.[1–6] Both mechanisms are likely to be operative; otherwise, the increase in B-ring radicals cannot be easily explained; but the second is definitely the key to the change of proportions in radical anions. It is most likely that the surge of A-ring radicals is such that the above equilibrium shifts to the left, increasing also the B-ring radicals concentration in this manner. That the latter is the case is confirmed by the pecan tannin spectra (where the proportion of B-ring radicals increases slightly just by this mechanism) [Fig. 4(a,b)]. It is also confirmed by the pine tannin spectra, where the relative surge of A-ring radicals is of such a magnitude that at the maximum of its intensity, it masks any other peak; however, the separate A- and B-rings' peaks can again be seen after the maximum of intensity is passed [Fig. 5(a,b)]. Notable in pine is that on addition of SiO_2, at maximum signal intensity, the proportion of A-ring radicals is slightly lower than the B-ring ones and that to balance this, the B-rings radicals decay is faster [Fig. 5(a,b)] to redress the equilibrium. This is again an indication that the heterocycle ring opening supersedes, both through base- and silica-induced mechanisms, the normally easier interflavonoid bond cleavage, and that on top of it, the B-rings $\rightleftharpoons$ A-rings radicals equilibrium moves to the right in this case.

Mimosa, for the same considerations on pyran ring opening already presented for this tannin, does not show major changes between cases in which silica has been and has not been added [Fig. 3(a,b)]. It is evident in the case of mimosa tannin that the relative proportions of A- and B-ring radicals is of approximately 50 : 50, which is consistent with model compounds work on these materials.[12,30,31] Gambier tannin shows similar, but more easily observable trends to pecan [Fig. 6(a,b)]. Addition of SiO_2 to Sumach tannin causes the increase of one of the less common A-ring radical species [(peak at 3484–3485 gauss; Fig. 7(a,b)], possibly indicating the presence in this tannin of some unusual flavonoid structures. Catechin monomer, as expected, behaves very similarly to gambier tannin in regard to the relative proportion of A-ring radical anions, but also shows a lower proportion of A-ring radical anions, indicating that side reactions like the catechinic acid rearrangement are operative,[25] that the catechinic acid rearrangement not only might partly occur through a radical mechanism but that it might also follow a totally radical mechanism, at least under certain reaction conditions; and that the catechin used in Figure 8(a,c) appears to have undergone previous rearrangements which confuses the issue. Fresh catechin spectra, with and without SiO_2 addition, appear as in Figure 9(a,b),

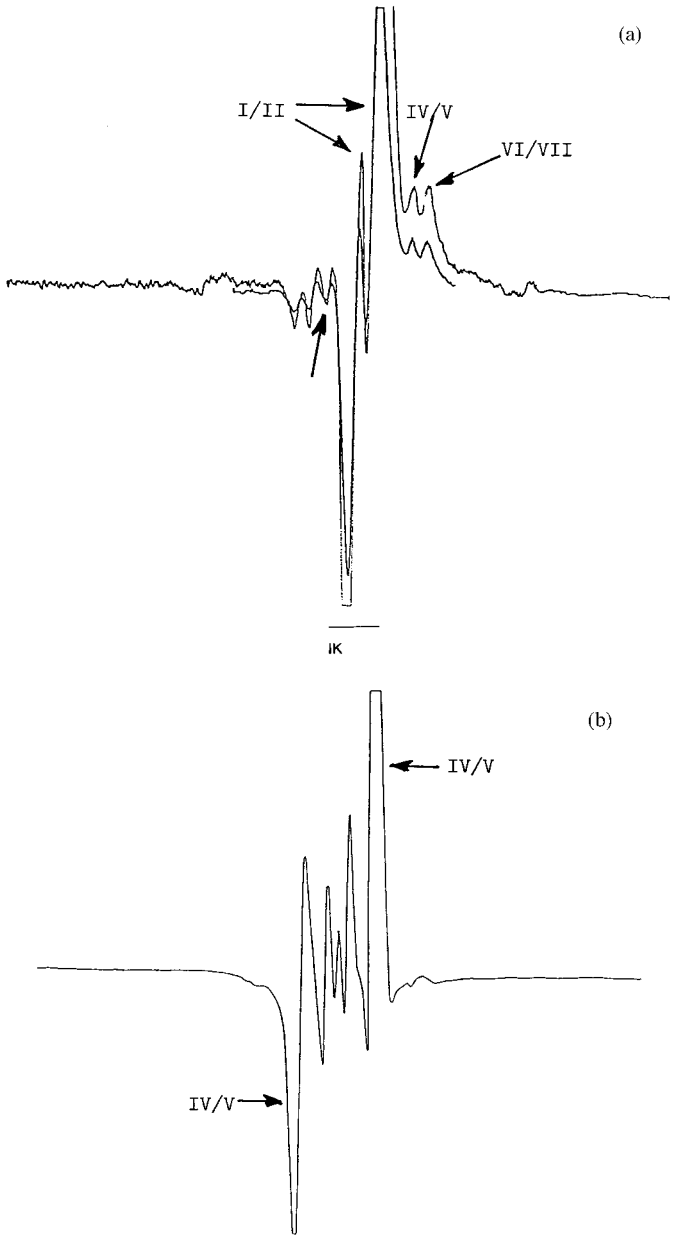

Figure 9 ESR spectra of (a) 15% fresh catechin monomer + base and (b) 15% fresh catechin monomer + base + 10% silica 5 min after base or base + silica addition. The corresponding radical anion couples are identified where possible.

where on addition of silica, the relative surge of A-ring radicals in relation to B-ring radicals is instead more evident.

The radical decay reaction appears to follow a first-order kinetic law (Table I) of the type $y = ae^{bt}$ for all tannins and also for the catechin monomer, although the latter is slightly more complex,[32] except for pine tannin and pecan tannin (Tables I and III). Pine and pecan tannin radical decay can also be modelled through the same kinetic law, but the fit is not good for all the ESR peaks.

It is worthwhile to discuss the case of the pecan tannin in more detail to illustrate the point. For all tannins, the radical formation reaction is so fast as to appear as instantaneous at ambient temperature (this with time = 1.5 min being taken as the start of the radical decay reaction and thus the maximum of the signal intensity). The intensity of the ESR signal then decreases exponentially as a function of time. In pecan tannin (as well as pine tannin) instead, the signal intensity starts to decrease more rapidly from its maximum, and then for a short

Table III Kinetic Law and Reaction Half-times of the Composite Radical Decay Reaction of Pecan Tannin

Peak (gauss)	Kinetic Law	Half-time (s)	Reaction Rate (s^{-1})
Pecan alone			
3479.6	$243.068\,(e^{-0.0062t} - e^{-0.3345t}) + 368.842e^{-0.6455t}$	2672	7.15×10^{-3}
3480.7	$171.224\,(e^{-0.0128t} - e^{-1.7432t}) + 378.384e^{-1.2794t}$	124	8.27×10^{-3}
3483.3	$240.651\,(e^{-0.0086t} - e^{-1.0826t}) + 389.789e^{-1.2989t}$	1471	10.60×10^{-3}
3484.4	$281.864\,(e^{-0.0026t} - e^{-0.3066t}) + 601.990e^{-0.6229t}$	120	8.02×10^{-3}
Average		1097	8.51×10^{-3}
Pecan + SiO_2			
3479.7	$163.838\,(e^{-0.0099t} - e^{-1.3648t}) + 916.773e^{-0.7501t}$	84	8.47×10^{-4}
3480.6	$144.094\,(e^{-0.0115t} - e^{-1.0670t}) + 1052.595e^{-0.1785t}$	77	9.57×10^{-4}
3483.3	$202.714\,(e^{-0.0138t} - e^{-1.3648t}) + 897.171e^{-0.7685t}$	92	7.72×10^{-4}
3484.5	$177.956\,(e^{-0.0075t} - e^{-0.7429t}) + 1580.6e^{-0.6382t}$	79	9.27×10^{-4}
Average		83	8.76×10^{-4}

time, it increases again to a limited extent, to again decrease permanently. The downward exponential curve then appears to have a sort of bulge (Fig. 10) for some of the peaks kinetics of pecan tannin without SiO_2 (3479.6 and 3484.4 gauss). This curve can be modelled through the combination of two different exponential functions, an ascending one and a descending one (Fig. 11; Table III). This points to the fact that two well distinct processes appear to be at work during these two tannins' radical decay reactions. While the main reaction clearly remains the radical decay reaction proper, it is of interest to consider what might be the reaction which causes the bulge in the curve. An increase in radical concentration well in the middle of the course of the radical decay reaction step can follow from four causes.

1. A temporary increase in the colloidal level of the system due to the autocondensation of the tannin produces polyflavonoids of higher DP_n. This would cause residual silica to restart the first step of the reactions for some units in which pyran ring opening

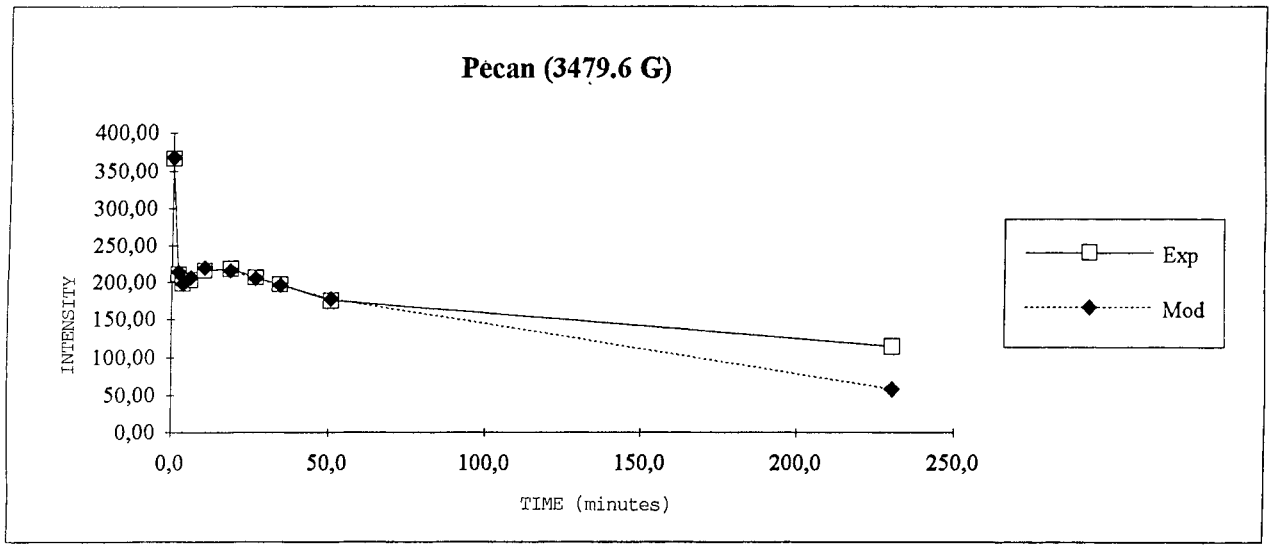

Figure 10 Radical decay reaction of pecan tannin + base as a function of time followed through the intensity variation of the 3479.6 gauss peak. Note the bulge between 10 and 30 min of reaction. Experimental points and complex kinetic law model are compared.

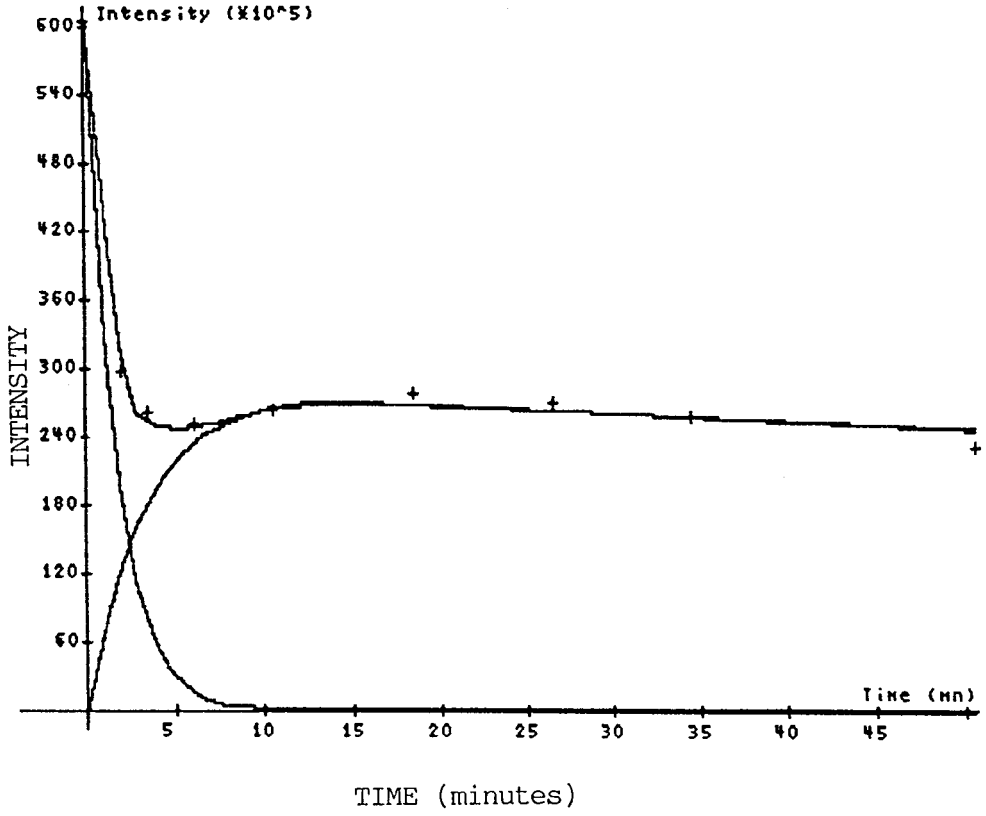

Figure 11 Modeling the complex experimental kinetics of pecan tannin + base. Curve (1) signal intensity = $a(e^{-bt} - e^{-ct})$. Curve (2) signal intensity = de^{-gt}. Curve (3) signal intensity = $a(e^{-bt} - e^{-ct}) + de^{-gt}$ (sum of curves 1 and 2).

might not have occurred, or might have been more difficult, due to the more favorable colloidal, micellar conditions created with the start of the polymerization. The effect would only be temporary.

2. It is safe to assume that the first step of the reaction still proceeds, albeit at a very much reduced rate, at the start of the second step of the reaction. As the second step of the reaction is particularly fast in these two tannins, the increased sharpness of the descending curve might reveal the still ascending curve of the first step of the reaction.
3. The presence of the B ⇌ A radicals equilibrium. If the A radicals decrease in concentration so fast, the equilibrium is capable of shifting towards the right to restore the A radicals concentration. This would imply that the A radicals concentration decays faster than that of the B radicals. There is some indication for this, mainly in the case of the gambier tannin (Table I), and for some but not all of the peaks of pine and pecan tannin. This shows that this is indeed a contributory factor but that it is not the only process at play.
4. A competitive reaction is present; i.e., the catechinic acid or another rearrangement gives an unstable product, which then recreates the original radical, which is then addressed down the more favorite reaction path.

With the data available, it is not possible to say for certain which of these processes are at work. It is possible that, to a different extent, all the causes just outlined contribute to the bulge in the curve.

From Table II, it is interesting to note that the rate of radical decay, when passing from SiO_2 absent to SiO_2 present systems, increases. This increase is more evident for some tannins than for

others. The order of decreasing intensity of the effect is as follows:

$$\text{Catechin} \gg \text{Mimosa} > \text{Pine} = \text{Pecan} > \text{Quebracho} > \text{Gambier} \gg \text{Sumach.}$$

It is of interest to understand what factors are at play to determine the above order of decreasing signal intensity for the different tannins. In Table II, the number-average degree of polymerization (DP_n) of these tannins, where known, is also reported.[19] The value of DP_n appears clearly to be inversely proportional to the increase in rate of radical decay on addition of SiO_2. All tannins and the catechin monomer, except gambier (and sumach, for which DP_n is not known), appear to present their DP_n related to the SiO_2/no-SiO_2 rate ratio (Table II) through an expression of the following type:

$$\text{(silica/no-silica) rate ratio} = -0.3379\ DP_n + 3.3199$$

of coefficient of correlation $r = 0.996$. This means that the lower the DP_n, the stronger the effect of silica in accelerating the rate of decay of the radicals formed. Colloidal state and characteristics of the A- and B-ring structures of the different tannins were also correlated; but with the exception of a very small influence from the colloidal state, no influence of the structures could be found. Thus, it is only at parity of DP_n that the colloidal state shows a determining influence on the effect of silica on the rate of the second step of the total reaction, as it has already been reported.[6]

Equally, the actual radical decay rate, both in the presence or absence of silica, is different for different tannins. The order of decreasing radical decay rate is as follows:

$$\text{Sumach} \gg \text{Mimosa} > \text{Pine} > \text{Pecan} \gg \text{Quebracho} \gg \text{Gambier} \gg \text{Catechin.}$$

Here again, correlation of this scale indicates that only DP_n plays a significant role on the second step of the reaction, and that the colloidal state appears to become determinant only at parity of DP_n.[6] The relationship is

$$\text{radical decay rate } (s^{-1}) = -2.755\ DP_n + 21.006$$

with coefficient of correlation $r = 0.93$. Only mimosa, pine, pecan, and quebracho tannins, however, follow this relationship. Gambier tannin and catechin monomer do not appear to follow it, and the necessary data for sumach are not available. This relation for the four most important commercial tannins indicates that the lower the DP_n of the tannin, the faster its radical decay rate. This implies that the more polymerized the tannin, the greater the radical stability and, hence, the greater the possible delocalization of the radical site. This is an interesting concept, as it means that a polyflavonoid tannin is able to function, to an extent, as a complete conjugated system, an idea which has not been advanced before.

The finding that the structure of the flavonoid repeating unit of tannins has very little influence on the second step of the reaction in the radical mechanism is again proof that an ionic mechanism is at work at the same time: gel time results[1] indicate that the scale of autocondensation rate is

$$\text{Pecan} = \text{Pine} > \text{Mimosa} > \text{Quebracho} \gg \text{Catechin}$$

where, clearly, both DP_n and particularly nucleophilicity of the A- and B-rings, hence the structure of the unit, are the main contributory factors and where colloidal state might not be. The radical reaction is then important for the first step of the reaction, the pyran ring opening; while for the second step of the reaction, both radical and ionic mechanisms, particularly the latter, appear to be important. Considering that both radical and ionic mechanisms[1,6] have been shown to be operative for the first step of the reaction, the question that needs to be addressed for the second reaction step is whether the radical decay reaction is really an important contributor to the condensation step proper, or is it unrelated to it (hence, it is only a side reaction) and condensation proceeds, after both ionic and radical pyran ring opening, only by an ionic mechanism. With the data presently available, it is not possible to say.

What it is possible to do, however, is to expand, from Table III, the interesting experience with pecan tannin. Comparing Tables III and I for pecan tannin, it becomes evident that while addition of silica shortens the half-time of reaction in all cases, hence makes the radical decay faster, this is not as clearly apparent from the reaction rate in s^{-1} (Table III). The reaction rate in s^{-1} is only an expression of the decay rate in intensity units

per second divided by the maximum intensity of the signal (in intensity units). The fact that in the silica case, this apparent reaction rate is just comparable or only marginally faster, indicates that a simple radical decay reaction occurs, but also that an apparent radical formation reaction, composed of both an intense radical formation surge and of another type of radical decay reaction (Fig. 11) is at work (the kinetic law is the combination of three exponential expressions). It also means that both for pecan tannin for which the real complexity of the whole reaction fortunately becomes visible, and for the other tannins, for which the same processes are likely to also be at work although they are not clearly visible, the real total system of radical decay reactions is considerably more complex than that presented. It also indicates that if radical decay is a consequence of different parallel reactions, only the main part of them are likely to lead to autocondensation; the others leading along different paths of reaction. It also indicates that for the total autocondensation to be as fast as it appears at the macroscopic level, an important component, or possibly the main component, of the second reaction step is ionic and hence not detectable by ESR.

Hydrolyzable tannins, such as tara, chestnut, and oak tannins, composed of simple low reactivity and nonpolymeric phenols such as gallic, digallic, and ellagic acid,[14] while presenting a phenoxide radical response in alkaline environment, as any phenol, do not present any radical surge mechanism by addition of silica. Furthermore, their ESR phenoxide signal does not resolve in a fine structure, as shown in Figure 12. They resolve in gallic acid phenoxide radicals in resonance (the equivalent of just a flavonoid B-ring peaks, or of pyrogallol[13] only) with just oak tannin, showing that it contains a minor proportion of flavonoids on top of the bulk of hydrolyzable tannins. This indicates conclusively that the mechanisms outlined for polyflavonoid tannins are characteristic to the flavonoid structure and that the silica and Lewis acids effect is localized at the pyran ring ether oxygen.

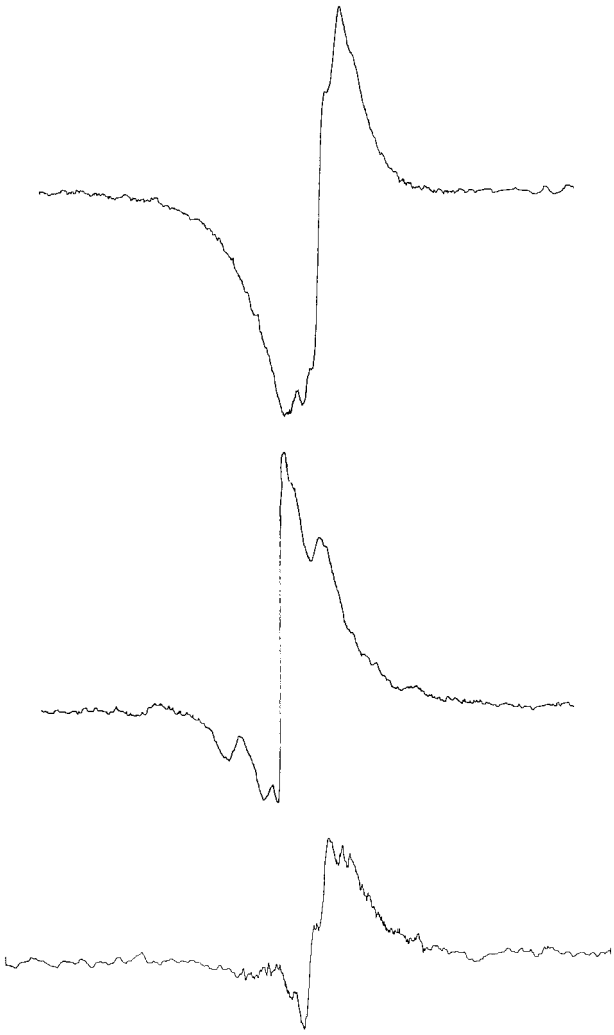

Figure 12 ESR spectra of three different hydrolyzable tannins: (a) chestnut tannin, (b) oak tannin, and (c) tara tannin, showing the lack of fine structure of the phenoxide radical signal for hydrolyzable tannins.

CONCLUSIONS

In conclusion, induced tannin autocondensations are catalyzed by both base attack on the flavonoids B-rings hydroxyls as well as by silica and other weak Lewis acids attack at the flavonoid pyran oxygen to form radical anions. The latter reaction is of such an intensity that the A-ring radicals surge immediately to a much higher proportion than the B-ring radicals. The latter's surge follows through shifting to the left of the B $\rightleftharpoons$ A radical species equilibrium and is mainly a consequence of the A-rings radical surge, which drives the reaction.

Different radical-anion species can be clearly identified from ESR spectra and the relative movements of the equilibria monitored. The intensity of the ESR peaks refers to the first step of the reaction, namely radical-anions formation, while the radical decay rate refers to the second reaction step, namely the condensation reaction proper. The rates of the two reaction steps were found to depend, by a different extent for the two

steps, from the colloidal level of the tannin solution, from the tannin DP_n and from the structure of the particular tannin involved, with the first two appearing to be somewhat more important. It is, however, the combination of these influences that determines the total observable effect for each type of polyflavonoid tannin, leading to a different characteristic behavior for each of the tannins examined. Again, both ionic and radical mechanisms appear clearly to be at work for both the two steps of the reaction, with the second step appearing to be rather a complex of different radical reactions and, hence, diminishing the radical mechanism importance in the condensation step proper, and with the ionic mechanism appearing, by default, to be the more important one in regard to the condensation step proper. For the first step of the reaction, both radical and ionic mechanisms appear instead to be of considerable importance.

REFERENCES

1. N. E. Meikleham, A. Pizzi, and A. Stephanou, *J. Appl. Polym. Sci.,* **54,** 1827 (1994).
2. A. Pizzi, N. E. Meikleham, and A. Stephanou, *J. Appl. Polym. Sci.,* **55,** 929 (1995).
3. A. Pizzi and N. E. Meikleham, *J. Appl. Polym. Sci.,* **55,** 1265 (1995).
4. A. Pizzi and P. Tekely, *J. Appl. Polym. Sci.,* **56,** 633 (1995).
5. A. Merlin and A. Pizzi, *J. Appl. Polym. Sci.,* **59,** 945 (1996).
6. E. Masson, A. Merlin, and A. Pizzi, *J. Appl. Polym. Sci.,* **60,** 263 (1996).
7. A. Pizzi, N. E. Meikleham, B. Dombo, and W. Roll, *Holz Roh Werkstoff,* **53,** 211 (1995).
8. A. Pizzi, *Advanced Wood Adhesives Technology,* Marcel Dekker, New York, 1994.
9. A. Pizzi, W. Roll, and B. Dombo, Deutscheland Patentanmeldung P 44 06 825.5; European Pat. 94 112177.4 (0 648 807 A1) (1995).
10. A. Pizzi and A. Stephanou, *J. Appl. Polym. Sci.,* **50,** 2105 (1993).
11. L. J. Porter, in *Plant Polyphenols,* R. W. Hemingway and P. E. Laks, Eds., Plenum, New York, 1992.
12. J. A. Kennedy, M. H. G. Munro, H. K. J. Powell, L. J. Porter, and L. Y. Foo, *Austr. J. Chem.,* **37,** 885 (1984).
13. B. H. Bielski and J. M. Gebicki, *Atlas of Electron Spin Resonance Spectra,* Academic Press, New York, 1967.
14. A. Pizzi, in *Wood Adhesives Chemistry and Technology,* A. Pizzi, Ed., Marcel, Dekker, New York, 1983, Chap. 4.
15. A. Pizzi and A. Stephanou, *Holzforschung und Holzverwertung,* **45(2),** 30 (1993).
16. S.-R. Kim, K. Saratchandra, and D. E. Mainwaring, *J. Appl. Polym. Sci.,* **56,** 905 (1995).
17. S.-R. Kim, K. Saratchandra, and D. E. Mainwaring, *J. Appl. Polym. Sci.,* **56,** 915 (1995).
18. S.-R. Kim and D. E. Mainwaring, *Holzforschung,* **50,** 42 (1996).
19. D. Thompson and A. Pizzi, *J. Appl. Polym. Sci.,* **55,** 107 (1995).
20. M. Fechtal and B. Riedl, *Holzforschung,* **47,** 349 (1993).
21. Leather Industries Research Institute, *Modern Applications of Mimosa Extract,* Grahamstown, South Africa, 1965, pp. 34–35.
22. I. Abe, M. Funaoka, and M. Kodama, *Mokuzai Gakkaishi,* **33(7),** 582 (1987).
23. A. Pizzi and A. Stephanou, *J. Appl. Polym. Sci.,* **51,** 2109 (1994).
24. A. Pizzi and A. Stephanou, *Holz Roh Werkdtoff,* **52,** 218 (1994).
25. P. E. Laks and R. W. Hemingway, *J. Chem. Soc., Perkins Trans. I,* 465 (1987).
26. W. McKillip, private communic., 1994.
27. Silva Ledoga, S. Michele Mondovi, Italy, private communic., 1994–1995.
28. G.-P. Benevento, private communic., 1995.
29. D. G. Roux, D. Ferreira, H. K. L. Hundt, and E. Malan, *Appl. Polym. Symp.,* **28,** 335–353 (1975).
30. J. A. Kuhnle, J. J. Windle, and A. C. Waiss, *J. Chem. Soc. (B),* 613 (1969).
31. O. H. Jensen and J. A. Pedersen, *Tetrahedron,* **39,** 1609 (1983).
32. J. Thomas, *Logedic, Lissages,* Version 1.1, Bourges, France, 1989.